

Matrix Infrared Spectra and Density Functional Calculations for GaNO, InNO, and TlNO

Lester Andrews,* Mingfei Zhou,[†] and Xuefeng Wang[†]

University of Virginia, Department of Chemistry, McCormick Road, P.O. Box 400319, Charlottesville, Virginia 22904-4319

Received: April 25, 2000; In Final Form: June 27, 2000

Laser-ablated Ga, In, and Tl atoms react with NO during condensation in excess argon at 10 K to give one major product, which absorbs at 1578.5 cm⁻¹ for Ga, 1524.9 cm⁻¹ for In, and 1454.6 cm⁻¹ for Tl. Infrared spectra of ¹⁴N¹⁶O, ¹⁵N¹⁶O, ¹⁵N¹⁸O, and mixed isotopic samples show that this product is the metal nitrosyl MNO. Density functional calculations provide good agreement for ³Σ⁻ GaNO and InNO, but higher level MP2 calculations are required to explain the bent structure and decreased N–O frequency for ³A'' TlNO. Model DFT calculations are also reported for Li[NO] and Li[NO]Li.

Introduction

The emission of nitrogen oxides (NO_x) from combustion exhausts causes serious impacts on terrestrial ecosystems. The selective reduction of NO with methane on gallium- and indium-containing zeolite catalysts has been investigated.¹ Gallium-containing zeolites have been employed as the catalyst for aromatization of light hydrocarbons, and Ga⁺ has been proposed as the active site.² It is important to prepare the GaNO and InNO species to serve as models for the initially adsorbed species.

The aluminum analogue,³ AlNO, exhibits a nitrosyl absorption at 1644.3 cm⁻¹ although the major reaction product is AlON, which absorbs^{3,4} at 1282.1 cm⁻¹. The Ga, In, and Tl nitrosyl absorptions are expected to decrease steadily from the Al value as the larger valence p orbitals overlap less effectively with nitrogen. Laser ablation has been employed for a study of group 13 metal cyanide and isocyanide products, and density functional theory frequency calculations have provided valuable support.⁵ Similar investigations have been done for a large number of transition metal nitrosyls.^{6–10} We report here such a study for Ga, In, Tl, and NO.

Experimental and Theoretical Methods

The laser-ablation matrix isolation experiment and apparatus have been described in previous reports.^{11,12} Metal targets (Ga, In, Tl)⁵ positioned 2 cm from the cold window were ablated by focused 1064 nm radiation from a pulsed YAG laser. Nitric oxide (Matheson) samples were prepared after fractional distillation from a coldfinger; ¹⁵N₂O (MSD Isotopes, 99% ¹⁵N) was treated similarly; ¹⁵N¹⁸O (Isotec, 99.9% ¹⁵N, 98.5% ¹⁸O) was used as received. A Nicolet 750 FTIR instrument operating at 0.5 cm⁻¹ resolution (frequency accuracy ±0.1 cm⁻¹) with liquid nitrogen cooled HgCdTe detector was used to record spectra. The instrument was purged continuously with a Balston 75-20 compressed air dryer. Matrix samples were co-deposited on a 10 K CsI window and were temperature cycled from 10 K to allow diffusion and reaction of trapped species, and more spectra were collected.

Density functional theory (DFT) calculations were performed on potential product molecules using the Gaussian 94 program

system.¹³ Most calculations employed the hybrid B3LYP functional, but comparisons were done with the BP86 functional as well.^{14,15} The 6-311+G* basis set was used for Ga, N, and O atoms and LANL2DZ for In and Tl atoms.^{16–18} Additional higher level MP2 calculations were performed for GaNO, InNO, and TlNO. Geometries were fully optimized, and the vibrational frequencies computed using analytical second derivatives.

Results

Infrared spectra for each metal system contained the usual metal independent absorptions for NO, (NO)₂, NO₂, NO₂⁻, (NO)₂⁺, and (NO)₂⁻, which have been discussed previously.^{6–10,19–22}

Infrared Spectra. The major new absorption was observed at 1578.5 cm⁻¹ for the Ga and ¹⁴N¹⁶O reaction with 0.082 absorbance; a much weaker associated band was found at 3127.0 cm⁻¹ (0.0054 au). In addition, weak absorptions were observed for the gallium oxides GaOGaO, OGaO, and GaOGa, as described previously.²³ Figure 1 shows the spectrum for a 0.5% ¹⁵N₂O sample in argon: the new bands are shifted to 3069.2 and 1549.0 cm⁻¹; stepwise annealing reduced these features and produced other bands believed due to aggregate species. In a ¹⁵N¹⁸O experiment these bands were further shifted to 2992.3 and 1510.0 cm⁻¹ as listed in Table 1. In a mixed ¹⁴N₂O + ¹⁵N₂O experiment, a weak doublet was observed at 3127.0, 3069.2 cm⁻¹ and no new bands were found in the congested region between 1578.5 and 1549.0 cm⁻¹.

The indium experiments behaved similarly. Figure 2 shows the spectrum with ¹⁴N¹⁶O and the new bands at 3020.9 and 1524.9 cm⁻¹. Note that these bands increase together on annealing to 30 K and then decrease on final annealing to 40 K. The same isotopic experiments were performed, and the shifted bands are listed in Table 1. Clear mixed isotopic doublets were observed for both bands with ¹⁴N₂O + ¹⁵N₂O. In addition, indium oxide absorptions were observed.²³

Thallium experiments gave two new peaks at 2885.6 and 1454.6 cm⁻¹, as shown in Figure 3. These bands almost doubled on annealing to 25 K, remained on ultraviolet photolysis, increased slightly on annealing to 35 K (full widths at half-maximum, 1.3 and 0.75 cm⁻¹, respectively), and decreased slightly on annealing to 40 K. The isotopic counterparts are listed in Table 1. The ¹⁴N₂O + ¹⁵N₂O experiment gave sharp

* Author for correspondence. Electronic mail: isa@virginia.edu.

[†] Permanent address: Laser Chemistry Institute, Fudan University, Shanghai, P. R. China.

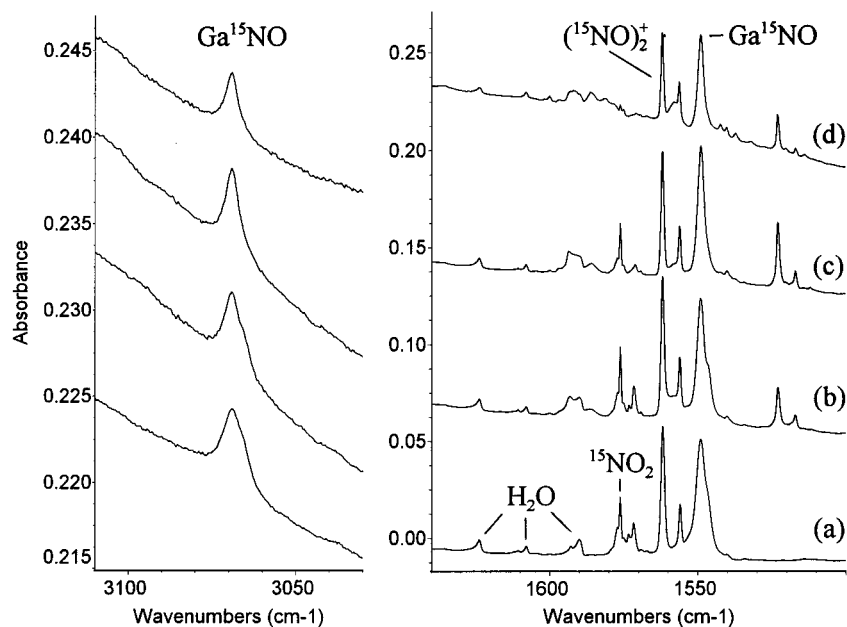


Figure 1. Infrared spectra in the 3110–3030 and 1640–1500 cm^{-1} regions for laser-ablated Ga co-deposited with 0.4% $^{15}\text{N}^{16}\text{O}$ in argon: (a) after deposition at 10 K for 1 h, (b) after annealing to 25 K, (c) after annealing to 30 K, and (d) after annealing to 40 K.

TABLE 1: Infrared Absorptions (cm^{-1}) from Laser-Ablated Ga, In, and Tl Atoms Co-deposited with NO in Excess Argon at 10 K

	$^{14}\text{N}^{16}\text{O}$	$^{15}\text{N}^{16}\text{O}$	$^{15}\text{N}^{18}\text{O}$	$R(14/15)$	$R(16/18)$	assignment
Ga + NO	3127.0	3069.2	2992.3	1.018 83	1.025 70	GaNO 2ν
	1732.6	1702.3	1657.1	1.017 80	1.027 28	$\text{Ga}_x(\text{NO})_y$
	1578.5	1549.0	1510.0	1.019 04	1.025 83	GaNO
	1550.3	1522.9	1482.4	1.017 99	1.027 32	$\text{GaNO}(\text{NO})_x$
	1542.8	1516.9	1474.6	1.017 07	1.028 69	$\text{GaNO}(\text{NO})_x$
	1191.0	1167.4	1141.7	1.020 22	1.022 51	$\text{Ga}^+(\text{NO})_2^-$
	1012.4	995.9	968.1	1.016 58	1.028 72	$\text{Ga}_x(\text{NO})_2$
	822.5	822.5	781.1	1.0000	1.053 00	Ga_2O
	796.3	796.3	752.2	1.0000	1.053 03	$\text{Ga}_2\text{O}(\text{NO})_x$
	748.1	739.2	714.1	1.012 04	1.035 15	$\text{Ga}_x\text{O}(\text{NO})_y$
	In + NO	3020.9	2966.9	2890.3	1.017 90	1.026 50
1524.9		1497.1	1458.2	1.018 57	1.026 68	InNO
1203.6		1179.6	1153.7	1.020 35	1.022 45	$\text{In}^+(\text{NO})_2^-$
1196.9		1172.9	1147.4	1.020 46	1.022 22	$\text{In}^+(\text{NO}_2^-)$ site
1030.7		1014.2	485.3	1.016 27	1.029 33	$\text{In}_x(\text{NO})_2$
517.9		503.6	501.5	1.028 40	1.004 19	?
Tl + NO	2885.6	2835.9	2759.6	1.017 53	1.027 65	TlNO 2ν
	2881.3	2831.7	2755.6	1.017 52	1.027 62	site
	1454.6	1429.3	1390.6	1.017 70	1.027 83	TlNO
	1452.6	1427.4	1388.7	1.017 65	1.027 87	TlNO site
	1239.3	1214.3	1187.5	1.020 59	1.022 57	$\text{Ti}^+(\text{NO}_2^-)$
	1028.4		983.6			$\text{Ti}_x(\text{NO})_2$

isotopic doublets for both absorptions. In addition, weak thallium oxide absorptions, mainly Tl_2O , from the target surface were observed.²⁴

Calculations. DFT/B3LYP calculations were performed for GaNO, InNO, and TlNO in triplet and singlet states. The results for GaNO are given in Table 2. The $^3\Sigma^-$ state is the global minimum, and the $^3A''$ side-bound state converged to the $^3\Sigma^-$ end-bound state. Computed frequencies are listed in Table 3. The BP86 calculation found $^3\Sigma^-$ GaNO 1.2 kcal/mol below $^3\Sigma^-$ GaON and lower 1606.0 and 1245.8 cm^{-1} nitrosyl frequencies, respectively, for both states. Singlet states are higher in energy.

Analogous calculations were done for InNO and TlNO using the LANL2DZ effective core potential for the metals and the D95* and 6-311+G* basis sets for N and O, and the results are presented in Table 4. The global minimum for both species is $^3\Sigma^-$, the $^3A''$ states converged to $^3\Sigma^-$ for both metals, and the $^1A'$ states were higher in energy. Similar calculations were done for GaNO, InNO, and TlNO at the MP2 level, and the

TABLE 2: Relative Energies and Geometries Calculated (B3LYP/6-311+G*) for GaNO and LiNO Isomer States

molecule	state	relative energy (kcal/mol)	geometry (\AA , deg)
GaNO	$^3\Sigma^-$	0	Ga–N, 1.985; N–O, 1.199; linear
GaON	$^3\Sigma^-$	+9.1	Ga–O, 1.920; O–N, 1.263; linear
$\text{Ga}[\text{NO}]^a$	$^1A'$	+17.7	Ga–N, 2.176; Ga–O, 2.243; N–O, 1.225
GaNO	singlet	+23.1	Ga–N, 2.032; N–O, 1.186; linear
GaON	singlet	+38.6	Ga–O, 2.035; O–N, 1.212; linear
NGaO	$^3\Sigma^-$	+53.3	N–Ga, 1.877; Ga–O, 1.661; linear
LiNO	$^3\Sigma^-$	0	Li–N, 1.717; N–O, 1.215; linear
$\text{Li}[\text{NO}]^b$	$^3A''$	+1.4	Li–N, 1.888; Li–O, 1.813; N–O, 1.270
LiON	$^3\Sigma^-$	+5.4	Li–O, 1.638; O–N, 1.269; linear
$\text{Li}[\text{NO}]$	$^1A'$	+15.8	Li–N, 1.847; Li–O, 1.773; N–O:1.248
LiNO	singlet	+25.4	Li–N, 1.729; N–O, 1.201; linear
LiON	singlet	+38.2	Li–O, 1.660; O–N, 1.240; linear

^a The triplet $\text{Ga}[\text{NO}]$ converged to triplet GaNO. ^b Mulliken charges: Li (+0.444), N (−0.245), O (−0.199). The $^3A'$ state is the global minimum state with the BP86 functional, and $^3\Sigma^-$ LiNO is +5.6 kcal/mol and $^3\Sigma^-$ LiNO is +21.3 kcal/mol.

results are summarized in Table 5. In agreement with B3LYP, GaNO and InNO have the linear $^3\Sigma^-$ ground states; however, TlNO adopts the bent $^3A''$ ground state. At the MP2 level, the $^3\Sigma^-$ state for TlNO has a negative bending frequency and the converged $^3A''$ state is bent with a 150.2° Ti–N–O angle and 0.5 kcal/mol lower in energy. Still higher level calculations will be required to describe TlNO. It is possible that spin–orbit coupling will be required to improve the calculations for TlNO.

Since the strong nitrosyl vibration for GaNO, InNO, and TlNO falls in the region observed for the nitrosyl vibration^{19,25,26} of $\text{Li}[\text{NO}]$, this ionic molecule was also computed for comparison. Although the $^3\Sigma^-$ end-bonded LiNO state is 1.4 kcal/mol lower than the $^3A''$ side-bonded $\text{Li}[\text{NO}]$ state, the 1393.4 cm^{-1} frequency and isotopic frequency ratios for the $^3A''$ state fit the experimental values (1352 cm^{-1} and $^{14}\text{NO}/^{15}\text{NO}$ ratio 1.017 61) much better than the computed $^3\Sigma^-$ state results. The lithium stretching mode predicted by B3LYP at 680.0 cm^{-1} and the −2.0 and −3.8 cm^{-1} ^{15}N and ^{18}O shifts are compatible with the observed (651.4 cm^{-1} , −1.0 and −5.6 cm^{-1}) values. Although $^3\Sigma^-$ LiON is only 4.0 kcal/mol higher than the $^3A''$ ring $\text{Li}[\text{NO}]$ structure, and the calculated 1408.3 cm^{-1} nitrosyl

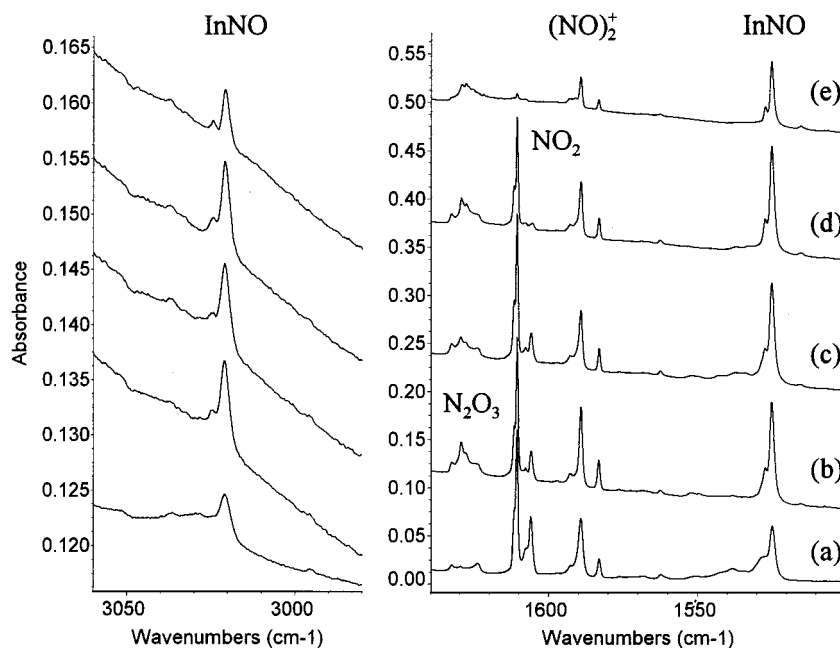


Figure 2. Infrared spectra in the 3060–2980 and 1640–1500 cm^{-1} regions for laser-ablated In co-deposited with 0.4% $^{14}\text{N}^{16}\text{O}$ in argon: (a) after deposition at 10 K for 1 h, (b) after annealing to 25 K, (c) after broad-band photolysis for 15 min, (d) after annealing to 30 K, and (e) after annealing to 40 K.

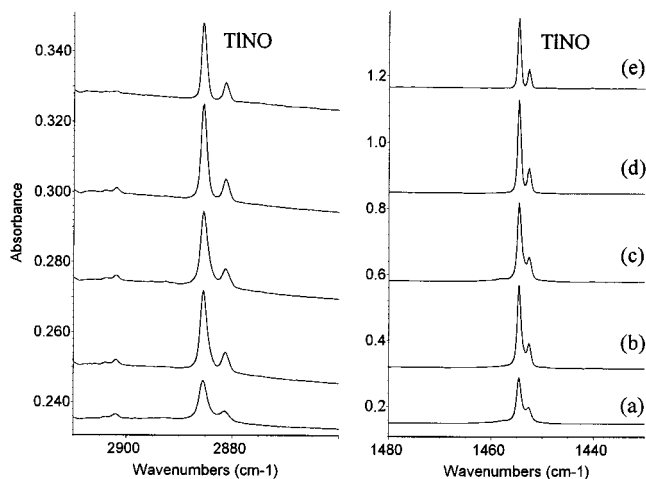


Figure 3. Infrared spectra in the 2910–2860 and 1480–1430 cm^{-1} regions for laser-ablated Tl co-deposited with 0.4% $^{14}\text{N}^{16}\text{O}$ in argon: (a) after deposition at 10 K for 1 h, (b) after annealing to 25 K, (c) after broad-band photolysis for 15 min, (d) after annealing to 30 K, and (e) after annealing to 40 K.

frequency is reasonable, the isotopic frequency ratios enhance the central atom participation, and this is not in agreement with experiment. The $^1\text{A}'$ ring isomer is 14.4 kcal/mol higher than the $^3\text{A}''$ ring, and the computed frequencies are higher and incompatible with the observed (1352, 651 cm^{-1})^{25,26} values. The BP86 functional was also employed for calculating the LiNO states, and $^3\text{A}''$ is the global minimum. The computed frequencies, 1326.5 cm^{-1} (101 km/mol) and 652.8 cm^{-1} (122 km/mol) are much closer to the observed values as expected. Thus, we conclude that lithium nitroxide is the side-bound highly ionic species described previously.^{19,26}

Calculations were performed for the dimetal species Li[NO]Li and In[NO]In at the BPW91 level, and the results are given in Table 6. Agreement with the three strongest infrared bands of Li[NO]Li at 886, 796, and 415 cm^{-1} is excellent.²⁶ The isotopic shifts define these vibrations as N–O stretching, and b_2 and a_1 Li–NO stretching modes.

Discussion

The new Ga, In, and Tl nitrosyls will be assigned on the basis of isotopic shifts and comparison to DFT isotopic frequency calculations.

GaNO. The 1578.5 and 3127.0 cm^{-1} absorptions are assigned to the nitrosyl fundamental and overtone of GaNO. The overtone is 30.0 cm^{-1} less than $2 \times 1578.5 = 3157.0 \text{ cm}^{-1}$, which is appropriate for anharmonicity. For AlNO, the overtone (3264.0 cm^{-1}) is 24.6 cm^{-1} lower than double the fundamental (1644.3 cm^{-1}),³ and for NO the overtone (3715.5 cm^{-1}) is 28.1 cm^{-1} lower than double the fundamental. The isotopic frequency ratios are characteristic of a N–O vibration. The $^{14}\text{NO} + ^{15}\text{NO}$ experiment reveals a clear 3127.0–3069.2 cm^{-1} mixed isotopic doublet, and although the 1500 cm^{-1} region contains many absorptions, no extra bands appear between 1578.5 and 1549.0 cm^{-1} ; hence, one NO submolecule is involved in these vibrations. The decrease in the strong Ga^{15}NO fundamental at 1549.0 cm^{-1} on annealing (Figure 1) strongly suggests that one Ga atom is involved. Therefore, the new molecule is identified as GaNO.

The DFT and MP2 calculations confirm that the 1578.5 cm^{-1} band is due to the $^3\Sigma^-$ ground state of GaNO. First the computed nitrosyl frequencies (1662.8 cm^{-1} , B3LYP, scale factor 0.947; 1606.0 cm^{-1} , BP86, scale factor 0.977; 1613.3 cm^{-1} , MP2, scale factor 0.978) support the assignment. These scale factors are compatible with other computations.²⁷ The calculated nitrosyl frequencies (Table 3) for the next two states $^3\Sigma^-$ GaON and $^1\text{A}'$ Ga[NO] are not in agreement with experiment. Of more importance, the observed isotopic frequency ratios, $^{14}\text{NO}/^{15}\text{NO}$ 1.0190, $^{15}\text{N}^{16}\text{O}/^{15}\text{N}^{18}\text{O}$ 1.0258, which are characteristic of the normal vibrational mode, are in excellent agreement with ratios 1.0191, 1.0258 computed for $^3\Sigma^-$ GaNO but not with ratios 1.0178, 1.0288 computed for $^3\Sigma^-$ GaON or ratios 1.0181, 1.0283 for $^1\text{A}'$ Ga[NO]. The normal mode for $^3\Sigma^-$ GaNO involves more nitrogen motion between Ga and O than in NO itself, and the normal modes for $^3\Sigma^-$ GaON and $^1\text{A}'$ Ga[NO] have different relative amounts of N and O character and different isotopic frequency ratios. Hence, isotopic frequency ratios as a descrip-

TABLE 3: Isotopic Frequencies (cm⁻¹), Intensities (km/mol), and Frequency Ratios Calculated (B3LYP/6-311+G*) for the Structures Described in Table 2

	14-16	15-16	15-18	R(14-16/ 15-16)	R(15-16/ 15-18)
LiNO	225.6(35)	221.0(34)	218.6(36)	1.0208	1.0110
³ Σ ⁻	725.7(169)	724.7(168)	718.0(167)	1.0014	1.0093
	1670.6(164)	1638.0(162)	1599.0(143)	1.0199	1.0244
Li[NO]	352.5(25)	348.4(26)	342.1(26)	1.0118	1.0184
³ A''	680.0(139)	678.0(137)	674.2(137)	1.0029	1.0056
	1393.4(97)	1368.9(96)	1330.9(87)	1.0179	1.0286
LiON	184.6(41)	183.5(42)	177.7(41)	1.0060	1.0326
³ Σ ⁻	769.9(142)	765.3(139)	763.8(140)	1.0060	1.0020
	1408.3(61)	1387.2(64)	1344.4(56)	1.0152	1.0318
Li[NO]	572.2(53)	566.2(53)	555.0(53)	1.0106	1.0202
¹ A'	714.6(71)	711.8(70)	708.7(70)	1.0039	1.0044
	1447.5(137)	1421.7(135)	1382.9(124)	1.0181	1.0281
LiNO	250.6(40)	245.5(39)	242.9(40)	1.0208	1.0107
singlet	292.8(21)	286.8(20)	283.7(22)	1.0209	1.0109
	712.2(101)	710.9(99)	705.0(100)	1.0018	1.0084
	1690.0(411)	1657.6(401)	1616.8(368)	1.0195	1.0252
LiON	187.2(28)	186.0(29)	180.1(28)	1.0065	1.0328
singlet	288.2(8)	286.3(9)	277.2(8)	1.0066	1.0328
	740.5(85)	737.0(86)	734.6(84)	1.0047	1.0033
	1437.2(160)	1414.0(149)	1372.0(146)	1.0164	1.0306
GaNO	50.8(5)	49.2(4)	49.2(4)	1.0325	1.0000
³ Σ ⁻	347.1(83)	343.5(81)	335.7(78)	1.0105	1.0232
	1662.8(242)	1631.6(241)	1589.5(215)	1.0191	1.0265
GaON	87.6(3)	87.4(3)	83.0(3)	1.0023	1.0530
³ Σ ⁻	386.2(81)	381.7(79)	373.8(76)	1.0118	1.0211
	1253.6(0.01)	1231.7(0.04)	1197.2(0.1)	1.0178	1.0288
Ga[NO]	265.0(24)	264.7(24)	253.4(22)	1.0011	1.0446
¹ A'	396.1(36)	385.1(35)	383.9(34)	1.0286	1.0031
	1498.5(143)	1471.9(139)	1431.4(131)	1.0181	1.0283
GaNO	36.9(0.3)	35.2(3)	36.2(0.3)	1.0483	
singlet	49.6(29)	47.8(27)	48.2(27)	1.0377	
	308.8(47)	305.5(45)	298.8(44)	1.0108	1.0224
	1698.6(405)	1667.5(398)	1623.2(364)	1.0187	1.0273
GaON	128.1(0.1)	127.1(0.1)	121.7(0.1)	1.0079	1.0444
singlet	159.5(12)	158.1(12)	151.6(11)	1.0089	1.0429
	275.9(15)	273.0(15)	266.9(14)	1.0106	1.0229
	1434.9(366)	1408.1(348)	1371.6(337)	1.0190	1.0266
NGaO	153.5(35)	151.5(35)	148.7(32)	1.0132	1.0188
³ Σ ⁻	566.6(17)	550.4(16)	547.8(17)	1.0294	1.0047
	911.2(6)	910.8(7)	871.2(5)	1.0004	1.0455

tion of the normal mode provide additional evidence for the ³Σ⁻ GaNO identification and assignment.

InNO. The assignment for the 1524.9 and 3020.9 cm⁻¹ bands to the nitrosyl fundamental and overtone of ³Σ⁻ ground-state InNO follows in like fashion. The overtone bands are relatively

stronger (7.9% of fundamental compared to 6.6% for GaNO), and the fundamental region is free of other (NO₂ and (NO)₂⁺) absorptions so clean mixed isotopic doublets are observed, and the participation of one NO submolecule is confirmed. The sharp fundamental and overtone bands increase together on annealing to 30 K and decrease together on further annealing (Figure 2), suggesting that a single In atom is involved. The most stable two-In, one-NO species was calculated (Table 5), and the spectrum is very different from that observed and assigned to InNO. The nitrosyl fundamental (1524.9 cm⁻¹) is calculated for ³Σ⁻ ground-state InNO at 1641.1 cm⁻¹ (B3LYP/6-311+G*, ratios 1.018 87, 1.026 84, scale factor 0.929) and at 1595.1 cm⁻¹ (BP86/6-311+G*, scale factor 0.956), and at 1599.7 cm⁻¹ (MP2/D95*/LANL2DZ, scale factor 0.953), which is acceptable agreement. Note that the observed ¹⁴NO/¹⁵NO and ¹⁵N¹⁶O/¹⁵N¹⁸O frequency ratios 1.018 57 and 1.026 68 agree extremely well with the above ³Σ⁻ InNO values and not with the ratios 1.018 03 and 1.028 35 computed for the all-too-low 1270.2 cm⁻¹ mode for ³Σ⁻ InON.

TiNO. The 1454.6 and 2885.6 cm⁻¹ absorptions are assigned to the nitrosyl fundamental and overtone of TiNO. Sharp doublets are observed for both bands in the mixed ¹⁴NO + ¹⁵NO experiment, and the bands increase together on annealing to 30 K and decrease together on annealing to 35 and 40 K. Ultraviolet photolysis has no effect on this product species.

While the isotopic ratios ¹⁴NO/¹⁵NO and ¹⁵N¹⁶O/¹⁵N¹⁸O for TiNO, 1.017 70 and 1.027 83, are almost exactly the same as NO values, 1.017 94 and 1.027 72, these ratios are distinctly different from the isotopic frequency ratios (Table 1) for the GaNO and InNO molecules. The latter molecules involve more N and less O motion in the nitrosyl normal mode coupled to the metals than in NO itself, which is expected for linear molecules. The absorptions observed for TiNO are characteristic of an essentially uncoupled N–O normal mode, and a different structure must be considered for TiNO. Although the computed N–O frequency is reasonable, the ¹A' side-bonded structure is 17.2 kcal/mol higher in energy than the end-bonded ³Σ⁻ state, and the B3LYP frequency for the ³Σ⁻ state, 1607.6 cm⁻¹, is too high for the experimental value.

Accordingly, MP2 computations were done for TiNO, and a bent ³A'' ground state was found with a 1550.4 cm⁻¹ N–O frequency and ¹⁴NO/¹⁵NO and ¹⁵N¹⁶O/¹⁵N¹⁸O frequency ratios 1.018 79 and 1.026 99, respectively. Although the frequency

TABLE 4: Calculated (B3LYP/D95*/LANL2DZ) Relative Energies, Geometries, Frequencies, and Intensities for InNO and TiNO Isomer States

molecule	relative energy (kcal/mol)	geometry (Å, deg)	frequencies (cm ⁻¹) for ¹⁴ N ¹⁶ O (intensities, km/mol)
InNO ^a ³ Σ ⁻	0.0	In–N, 2.114; N–O, 1.215; linear	103.8(1), 319.0(49), 1669.4(294)
InON ^c ³ Σ ⁻	+7.5	In–O, 2.010; O–N, 1.279; inear	133.1(1), 283.2(15), 1273.0(151)
In[NO] ¹ A'	+17.6	In–N, 2.312; In–O, 2.301; N–O, 1.244	274.6(18), 390.0(20), 1486.6(154)
InNO singlet	+23.6	In–N, 2.165; N–O, 1.202; linear	75.0(2), 140.0(11), 285.7(24), 1704.4(487)
InON singlet	+38.2	In–O, 2.132; O–N, 1.230; linear	113.4(1), 190.8(3), 249.3(7), 1444.1(386)
NInO ³ A''	+65.6	N–In, 2.052; In–O, 1.771; ∠NInO, 179.7	131.5(33), 470.8(10), 761.1(4)
TiNO ^{a,d} ³ Σ ⁻	0.0	Ti–N, 2.360; N–O, 1.216; linear	97.5(3), 258.1(26), 1634.0(687)
TiON ³ Σ ⁻	+8.8	Ti–O, 2.302; O–N, 1.259; linear	104.2(2), 269.5(16), 1310.7(297)
Ti[NO] ^e ¹ A'	+17.2	Ti–N, 2.551; Ti–O, 2.553; N–O, 1.234	241.9(6), 362.5(17), 1508.5(388)
TiNO singlet	+21.8	Ti–N, 2.420; N–O, 1.201; linear	123.0(0), 138.6(11), 240.4(10), 1695.3(894)
TiON singlet	+34.8	Ti–O, 2.432; O–N, 1.216; linear	135.5(0), 187.0(4), 212.4(2), 1536.6(819)
NTiO ³ A''	+100.3	N–Ti, 2.297; Ti–O, 1.975; ∠NTiO, 179.0	140.2(17), 275.3(3), 620.5(32)

^a The triplet M[NO] converged to triplet MNO. ^b The 6-311+G* basis gave In–N, 2.148; N–O, 1.203 and the 52.5(9), 300.0(64), 1641.1(354) frequencies for ¹⁴N¹⁶O with the latter shifting to 1610.7 and 1568.6 cm⁻¹ for ¹⁵N¹⁶O and ¹⁵N¹⁸O. ^c The 6-311+G* basis gave this state +6.7 kcal/mol, In–O, 2.052; O–N, 1.264 and the 91.5(3), 322.7(61), 1270.2(6) frequencies for ¹⁴N¹⁶O with the latter shifting to 1247.7 and 1213.3 cm⁻¹ for ¹⁵N¹⁶O and ¹⁵N¹⁸O. ^d The 6-311+G* basis gave Ti–N, 2.398; N–O, 1.203 and the 24.9(18), 250.2(35), 1607.6(809) frequencies for ¹⁴N¹⁶O with the latter shifting to 1578.2 and 1536.2 cm⁻¹ for ¹⁵N¹⁶O and ¹⁵N¹⁸O. ^e The 6-311+G* basis gave this state +17.0 kcal/mol, Ti–N, 2.570; Ti–O, 2.609; N–O, 1.216 and the 219.6(7), 334. (37), 1508.1(487) frequencies for ¹⁴N¹⁶O with the latter shifting to 1481.1 and 1440.6 cm⁻¹ for ¹⁵N¹⁶O and ¹⁵N¹⁸O.

TABLE 5: Calculated (MP2/D95*/LANL2DZ) Relative Energies, Bond Lengths, Frequencies, and Intensities for GaNO, InNO, and TiNO Isomer States

molecule	rel. energy (kcal/mol)	bond lengths (Å)	frequencies (cm ⁻¹) ^a
GaNO ^b	0.0	Ga-N: 1.924 N-O: 1.232	1613.3(28), 1582.0, 1542.9 392.1(104), 388.3, 397.0 125.8(8), 122.7, 121.0
¹ A'	11.3	Ga-N: 2.108 Ga-O: 2.178 N-O: 1.274	1392.2(58), 1367.0, 1330.2 436.2(25), 424.3, 422.2 309.3(30), 308.9, 296.0
GaNO ^c	0.0	Ga-N: 1.953 N-O: 1.208	1598.1(71), 1567.1, 1528.6 407.7(132), 407.8, 392.3 63.1(15), 61.6, 60.7
¹ A'	10.4	Ga-O: 2.109 Ga-N: 2.209 N-O: 1.251	1362.7(57), 1338.2, 1302.0 446.2(42), 433.8, 432.8 284.7, 284.4, 271.9
InNO ^d	0.0	In-N: 2.088 N-O: 1.236	1599.7(52), 1569.0, 1529.8 347.8(93), 343.8, 334.7 104.1(9), 101.6, 100.1
¹ A'	11.9	In-N: 2.277 In-O: 2.332 N-O: 1.272	1389.1(102), 1364.0, 1327.2 414.2(22), 402.7, 399.9 283.6(24), 282.8, 270.5
TiNO ^e	0.0	Ti-N: 2.267 N-O: 1.241 ∠TiNO: 157.3°	1558.8(161), 1526.5, 1487.3 323.9, 318.7, 311.1 71.0, 69.5, 68.1
¹ A'	10.3	Ti-N: 2.437 Ti-O: 2.2523 N-O: 1.261	1382.0(356), 1357.0, 1320.5 395.3(17), 384.0, 381.2 266.9, 265.9, 253.8
TiNO ^c		Ti-N: 2.291 N-O: 2.222 ∠TiNO: 150.2°	1540.4(256), 1521.8, 1481.8 320.2(99), 314.0, 308.1 112.5(3), 110.5, 107.7

^a Frequencies for ¹⁴N¹⁶O isotope (intensity, km/mol), for ¹⁵N¹⁶O and ¹⁵N¹⁸O isotopes. ^b Mulliken charges: Ga(+0.66), N(-0.43), O(-0.23). ^c 6-311+G* basis sets for N and O. ^d Mulliken charges: In(+0.70), N(-0.44), O(-0.26). ^e Mulliken charges: Ti(+0.72), N(-0.40), O(-0.32).

TABLE 6: Calculated Geometries, Frequencies, and Intensities for Li[NO]Li and In[NO]In

molecule	geometry (Å)	frequencies, cm ⁻¹ (intensities, km/mol)
Li[NO]Li ^d	Li-N: 1.823	878.1(42), ^b 864.7, ^c 844.3, ^d 888.9 ^e
² A'', C _{2v}	Li-O: 1.766 N-O: 1.451	800.6(239), 794.9, 789.9, 844.3 647.9(36), 646.9, 643.3, 691.2 624.9(17), 618.4, 604.5, 640.3 399.0(151), 396.6, 393.5, 421.1 164.1(164), 163.4, 161.6, 173.1
In[NO]In	In-N: 2.233	919.4(6) ^b , 499.5(261), 313 (55), 158.0(4), 117.4(14), 78.3(3.0)
² A'', C _{2v}	In-O: 2.300 N-O: 1.390	

^a Mulliken charges: Li(+0.279), N(-0.239), O(-0.318). ^b ⁷Li/¹⁴N¹⁶O isotopes. ^c ⁷Li/¹⁵N¹⁶O isotopes. ^d ⁷Li/¹⁵N¹⁸O isotopes. ^e ⁶Li/¹⁴N¹⁶O isotopes.

and isotopic ratios fit better for the MP2-computed ³A'' state, we suspect that the observed molecule may be even more bent than the 150.2° MP2 angle. The MP2 calculations strongly suggest that TiNO is bent, in contrast to GaNO and InNO.

Other Absorptions. Each metal experiment exhibited absorptions, which appeared on annealing and are due to higher complexes. This is most pronounced with Ga where several such species are observed. Each metal also gave evidence for M⁺NO₂⁻ species in the 1190–1240 cm⁻¹ region, which are analogous to the alkali metal species.¹⁹

Finally, bands were observed at 1012.4 cm⁻¹ for Ga, 1030.7 cm⁻¹ for In, and 1028.4 cm⁻¹ for Ti, which showed triplet bands in mixed isotopic experiments for two equivalent NO sub-molecules. These bands are probably due to metal hyponitrite species, which will be investigated more fully.^{28,29}

Conclusions

Laser-ablated group 13 metal atoms react with NO to form metal nitrosyl molecules MNO. Although the AlNO and GaNO nitrosyls absorb in the 1600 ± 50 cm⁻¹ region typical of early transition metal nitrosyls,^{6–9} no higher nitrosyls are observed. Furthermore, the InNO and TiNO nitrosyl frequencies are lower, particularly TiNO, and more characteristic of group 1 and 2 nitrosyls, which are described as ionic species.^{26,30,31} Hence, as expected, group 13 metal nitrosyls are more like alkali and alkaline than transition metal nitrosyls.

Acknowledgment. We gratefully acknowledge N.S.F. support for this research under Grant CHE 97-00116.

References and Notes

- (1) Kikuchi, E.; Ogura, M.; Terasake, I.; Goto, Y. *J. Catal.* **1996**, *161*, 465.
- (2) Price, G. L.; Kanazirev, V. *J. Catal.* **1990**, *126*, 267.
- (3) The AlNO overtone was observed at (3270.5 cm⁻¹ site) 3264.0 cm⁻¹ with 15% of the intensity of the 1644.3 cm⁻¹ fundamental. The ¹⁵N¹⁸O and ¹⁵N¹⁶O isotopic values are (3207.8 cm⁻¹ site) 3201.4 cm⁻¹ and (3132.6 cm⁻¹ site) 3126.7 cm⁻¹, respectively.
- (4) Ruschel, G. K.; Ball, D. W. *High Temp. Mater. Sci.* **1997**, *37*, 63. At our request D. W. Ball checked his original spectra and found a weak 1644 cm⁻¹ band.
- (5) Lanzisera, D. V.; Andrews, L. *J. Phys. Chem. A* **1997**, *101*, 9660.
- (6) Zhou, M. F.; Andrews, L. *J. Phys. Chem. A* **1998**, *102*, 7452 (Cr + NO).
- (7) Zhou, M. F.; Andrews, L. *J. Phys. Chem. A* **1999**, *103*, 478 (V + NO).
- (8) Zhou, M. F.; Andrews, L. *J. Phys. Chem. A* **1998**, *102*, 10025 (Nb, Ta + NO).
- (9) Andrews, L.; Zhou, M. F. *J. Phys. Chem. A* **1999**, *103*, 4167 (Mo, W + NO).
- (10) Zhou, M. F.; Andrews, L. *J. Phys. Chem. A* **2000**, *104*, 3915 (Fe, Co, Ni + NO).
- (11) Burkholder, T. R.; Andrews, L. *J. Chem. Phys.* **1991**, *95*, 8697.
- (12) Hassanzadeh, P.; Andrews, L. *J. Phys. Chem.* **1992**, *96*, 9177.
- (13) Frisch, M. J.; Trucks, G. W.; Schlegel, H. B.; Gill, P. M. W.; Johnson, B. G.; Robb, M. A.; Cheeseman, J. R.; Keith, T.; Petersson, G. A.; Montgomery, J. A.; Raghavachari, K.; Al-Laham, M. A.; Zakrzewski, V. G.; Ortiz, J. V.; Foresman, J. B.; Cioslowski, J.; Stefanov, B. B.; Nanayakkara, A.; Challacombe, M.; Peng, C. Y.; Ayala, P. Y.; Chen, W.; Wong, M. W.; Andres, J. L.; Replogle, E. S.; Gomperts, R.; Martin, R. L.; Fox, D. J.; Binkley, J. S.; Defrees, D. J.; Baker, J.; Stewart, J. P.; Head-Gordon, M.; Gonzalez, C.; Pople, J. A. *Gaussian 94, Revision B.1*; Gaussian, Inc.: Pittsburgh, PA, 1995.
- (14) Lee, C.; Yang, E.; Parr, R. G. *Phys. Rev. B* **1988**, *37*, 785.
- (15) Perdew, J. P. *Phys. Rev. B* **1986**, *33*, 8822. Becke, A. D. *J. Chem. Phys.* **1993**, *98*, 5648.
- (16) McLean, A. D.; Chandler, G. S. *J. Chem. Phys.* **1980**, *72*, 5639.
- (17) Krishnan, R.; Binkley, J. S.; Seeger, R.; Pople, J. A. *J. Chem. Phys.* **1980**, *72*, 650.
- (18) Hay, P. J.; Wadt, W. R. *J. Chem. Phys.* **1985**, *82*, 299.
- (19) Milligan, D. E.; Jacox, M. E. *J. Chem. Phys.* **1971**, *55*, 3404.
- (20) Jacox, M. E.; Thompson, W. E. *J. Chem. Phys.* **1990**, *93*, 7609.
- (21) Strobel, A.; Knoblauch, N.; Agreiter, J.; Smith, A. M.; Nerder-Schatteburg, G.; Bondybey, V. E. *J. Phys. Chem.* **1995**, *99*, 872.
- (22) Andrews, L.; Zhou, M. F.; Willson, S. P.; Kushto, G. P.; Snis, A.; Panas, I. *J. Chem. Phys.* **1998**, *109*, 177.
- (23) Burkholder, T. R.; Yustein, J. T.; Andrews, L. *J. Phys. Chem.* **1992**, *96*, 10189.
- (24) Andrews, L.; Kushto, G. P.; Yustein, J. T.; Archibong, E.; Sullivan, R.; Leszczynski, J. *J. Phys. Chem. A* **1997**, *101*, 9077.
- (25) Andrews, W. L. S.; Pimentel, G. C. *J. Chem. Phys.* **1966**, *44*, 2361.
- (26) Tevault, D. E.; Andrews, L. *J. Phys. Chem.* **1973**, *77*, 1640 (Li + NO). Tevault, D. E.; Andrews, L. *J. Phys. Chem.* **1973**, *77*, 1646 (Na + NO).
- (27) Scott, A. P.; Radom, L. *J. Phys. Chem.* **1996**, *100*, 16502.
- (28) Kuhn, L.; Lippincott, E. R. *J. Am. Chem. Soc.* **1956**, *78*, 1820.
- (29) Andrews, L.; Liang, B., to be published.
- (30) Tevault, D. E.; Andrews, L. *J. Chem. Phys. Lett.* **1977**, *48*, 103.
- (31) Kushto, G. P.; Ding, F.; Liang, B.; Wang, X.; Citra, A.; Andrews, L. *J. Chem. Phys.* **2000**, *257*, 223.